Crossover of dynamical instability and chaos in the supercritical state

C. Cockrell*

School of Physics and Astronomy, Queen Mary University of London, London E1 4NS, United Kingdom

(Received 13 October 2020; accepted 24 November 2020; published 11 December 2020)

We calculate the maximal Lyapunov exponent for a bulk system of 256 Lennard-Jones particles in constant energy molecular dynamics simulations deep into the supercritical state. We find that the maximal Lyapunov exponent undergoes a crossover and that this crossover coincides with the dynamical crossover at the Frenkel line from liquid physics. We explain this crossover in terms of two different contributions to dynamical instability: diffusion in the liquidlike state below the Frenkel line and collisions in the gaslike state above. These results provide insight into the phase-space dynamics far from the melting line and densities where rare-gas approximation are inapplicable.

DOI: 10.1103/PhysRevE.102.062206

I. INTRODUCTION

Equilibration remains one of the major unanswered questions in nonequilibrium statistical mechanics [1], despite the phenomenal success and ubiquity of equilibrium statistical mechanics in physics. The measure-preserving (Liouvillean) dynamics of Hamiltonian systems prohibits the diffusive smoothing of the probability density function into its equilibrium form starting from an arbitrary initial state [1], but in *mixing* dynamical systems any subset of the phase space will, after enough time, uniformly explore the available phase space [2]. Phase (and time) averaged properties in a mixing system approach well-defined constants as $t \to \infty$ as any probability density spreads out to explore the entire phase space and becomes uncorrelated with its initial conditions at $t = 0$ [2].

The mixing property has its origins in dynamical instability [3], a measure of which is the Lyapunov spectrum [2]. Lyapunov spectra measure the rate of divergence of neighboring trajectories in phase space. Consider a point $\Gamma(0)$ in the phase space at time $t = 0$ and its perturbation in the phase-space direction i, $\Gamma(0) + \delta\Gamma_i(0)$. If the dynamics are unstable, then this perturbation will rapidly grow and erase correlations between the two trajectories. The state after time $t = \tau$ can be written $\Gamma(\tau) + \delta\Gamma(\tau)$, where $\Gamma(\tau)$ is the time-evolved unperturbed trajectory, and the time-evolved perturbation $\delta\Gamma(\tau)$ will, in general, spread into all phase-space dimensions. The Lyapunov exponents, λ_i are defined [4]

$$\lambda_i = \lim_{t\to\infty} \frac{1}{t} \log\left[\frac{|\,\delta\Gamma_i(t)\,|}{|\,\delta\Gamma_i(0)\,|}\right]. \tag{1}$$

The Lyapunov spectrum therefore defines the directions in which the phase-space contracts and expands under time evolution. The sum of the Lyapunov exponents is related to the phase-space contraction rate and thus vanishes for Liouvillean flows [4]. The presence of just one positive Lyapunov exponent signifies dynamical instability, and the perturbation size $\frac{|\delta\Gamma(t)|}{|\delta\Gamma(0)|}$ will be dominated by the largest positive Lyapunov exponent, Λ. We may therefore write

$$\Lambda = \lim_{t\to\infty} \frac{1}{t} \log\left[\frac{|\,\delta\Gamma(t)\,|}{|\,\delta\Gamma(0)\,|}\right], \tag{2}$$

assuming that we can ignore the contrived case where the initial perturbation is perpendicular to the fastest expanding phase-space direction. The Lyapunov spectrum will, in general, be functions of the phase space; however, for ergodic systems it can immediately be seen from Eq. (1) that the spectrum will be a constant for a given dynamical system.

Chaotic dynamics have received ample attention in physics beyond theoretical considerations. Lyapunov exponents have been used to calculate transport properties [5–8]. Additionally, the ability of digital computers to faithfully represent the dynamics of chaotic systems is an increasingly important question (for a particularly striking example of a digital computer's failure, see the recent work [9]), and the Lyapunov spectrum has been proposed as a natural measure of the deviation of the calculated trajectory from the "true" one [10].

In this work we study the maximal Lyapunov exponent (MLE) Λ of atomic Lennard-Jones (LJ) systems in the solid phase and liquid phase above and below the Frenkel line (FL) using molecular dynamics (MD) simulations. The FL separates two different dynamic regimes in the fluid phase: At temperatures below the line, atomic motion combines oscillation around quasiequilibrium positions with diffusive jumps ("liquidlike"); above the line, atomic motion is purely diffusive ("gaslike") [11–13]. See Fig. 1 for representative trajectories in these different states from MD simulations. This gives a practical criterion to calculate the FL based on the disappearance of the minima of the velocity autocorrelation function (VAF). The FL represents a crossover not only in dynamics but also in thermodynamics and structure [14–20]. The nature of the crossover at the FL is not yet well understood, and many interesting and competing phenomena

*c.j.cockrell@qmul.ac.uk

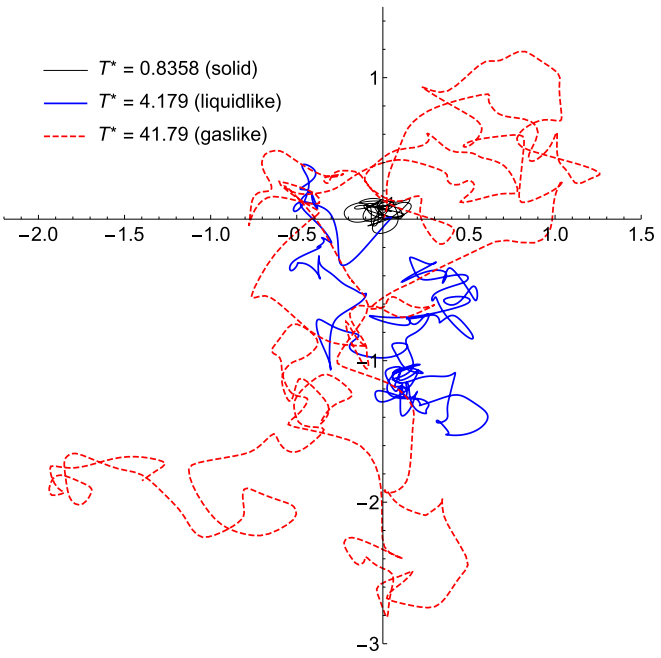

FIG. 1. Projected particle trajectories on the x-y plane (in reduced length units, see Table I) at a reduced concentration of 1.056 in the solid phase and the fluid phase below and above the Frenkel line.

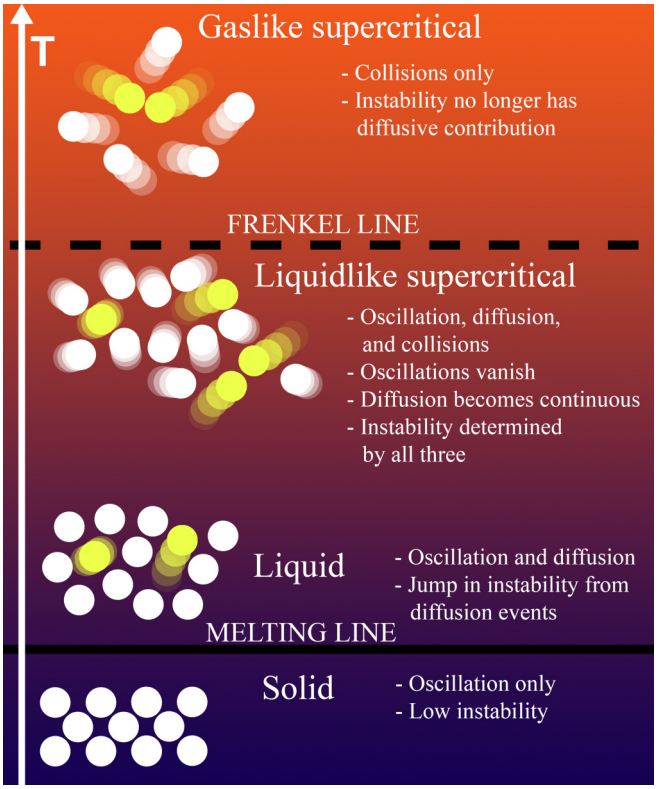

FIG. 2. Summary of our main results: Evolution of dynamical instability in condensed matter, from solids at low temperature to gaslike supercritical fluids at high temperature. The figure shows the dynamical regimes in each state of matter (oscillation, diffusion, collisions) and their relationship to the dynamical instability.

which separate "liquidlike" and "gaslike" states in supercritical fluids have been discovered [21–25]. Classification and stratification of the supercritical state therefore remains an open and exciting problem.

One of the seminal examples used in chaos theory is the Lorentz gas [26], which models an ideal gas in the dilute limit, and whose Lyapunov exponent is well known [4]. On the other hand, the Lyapunov spectrum of condensed phases have also been well studied in the condensed phase using MD simulations [27–31]. The behavior of Lyapunov spectra across phase transitions has been documented [28–35], exhibiting discontinuities in the MLE itself or its first derivative with respect to an order parameter. Phases are an ultimately macroscopic notion, but particle dynamics and phase-space properties like Lyapunov spectra can both provide a quantitative *microscopic* description of the phases and the transitions between them, motivating our line of inquiry.

In this paper we show that dynamically distinct states which the FL separates are also chaotically distinct. The MLE is known to change over the melting line so it stands to reason that dynamical changes in the supercritical state should have an effect on the MLE too. Specifically, the MLE experiences a change in its evolution with total system energy which coincides with the loss of atomic oscillation over the FL. This change in evolution is explained in terms of the a shift of chaotic dynamical events, from oscillation to diffusive jumps to ballistic collisions (see Fig. 2 for an overview).

II. METHODS

We consider a bulk system of 256 atoms with periodic boundary conditions interacting under the LJ potential:

$$V_{ij} = 4\epsilon\left[\left(\frac{\sigma}{r_{ij}}\right)^{12} - \left(\frac{\sigma}{r_{ij}}\right)^{6}\right], \tag{3}$$

where V_{ij} is the pair potential energy between atoms i and j, ϵ is the well depth, σ is the atomic radius, and r_{ij} is the radial distance between them. For the purpose of continuity, we have selected the LJ potential characterizing argon (see Table I), whose behavior across the FL has been well characterized [14,15,36]. We use the DL_POLY MD simulation package [37], which in the NVE ensemble uses the velocity-Verlet [38] integration algorithm. In simulations, we use time units of picoseconds (ps) and integration time steps between 10^{-3} and 10^{-5} ps, with none of our results displaying sensitivity on the choice of time step within this range. For analysis and discussion, we use the reduced time $t^* = t/\tau$ [$\tau = \sqrt{m\sigma^2/\epsilon} = 2.163$ ps] instead. Total energy is conserved to within 0.01% for all production runs.

TABLE I. Potential parameters used in the molecular dynamics simulations.

Parameter	Value
Mass (amu)	39.95
ϵ (eV)	0.01032
ϵ (K)	119.65
σ (Å)	3.4

TABLE II. Thermodynamic data for each system investigated: ρ, mass density; n, concentration (number density); T_F, temperature at the Frenkel line; $T_F^* = k_B T_F/\epsilon$, reduced temperature at the Frenkel line; E_F/N, energy per particle at the Frenkel line; $E_F^*/N = E_F/\epsilon N$, reduced energy per particle at the Frenkel line. k_B is Boltzmann's constant and ϵ is given in Table I. The reference energy is $E^*/N = 0$ at $n^* = 0.5917$ and $T^* = 0.5$ (20 K).

n^*	0.7101	0.8284	1.065
ρ (g/ml)	1.199	1.403	1.798
n (Å^{-3})	0 0.01807	0.02108	0.02710
T_F (K)	295	997	3850
T_F^*	2.45	8.33	32
E_F/N (eV)	−0.00432	0.116	0.650
E_F^*/N	5.28	16.9	69.0

Our initial configuration consisted of 256 argon atoms in a cubic cell arranged in an FCC crystal structure [39] with lattice constants of 6.049, 5.747, and 5.285 Å, corresponding to reduced concentrations ($n^* = n/\sigma^3$) of 0.7101, 0.8284, and 1.065 respectively. Mass and number densities in standard units are given in Table II. In order to generate structures corresponding to the target temperatures, the crystalline initial conditions were heated in the NVT ensemble using a fluctuating disspative (Langevin) thermostat for 2×10^5 MD time steps. The temperature ranged from 20 K in the crystalline state to 5000 K in the deep supercritical state, passing the melting line and Frenkel line. Temperature T is defined from equipartition as

$$T = \frac{2\overline{E_{\rm kin}}}{(3N-6)k_B}, \tag{4}$$

where $\overline{E_{\rm kin}}$ is the kinetic energy averaged over the trajectory, N is the number of atoms, and k_B is Boltzmann's constant. Near the melting line, we increased the density of temperature points to capture the sharp transition there. Relevant physical parameters in DL_POLY units and reduced LJ units are listed in Table II. The configurations generated in this heating stage were used as initial conditions for data collection in the NVE ensemble for 2×10^5 MD time steps. From this stage statistical data such as total energy, diffusion coefficients, and VAFs were collected.

The final configurations from NVE data collection were used as the initial configurations in the production runs where the MLEs were calculated. We calculated the MLE using the tangent space method [40]: At the beginning of the production run, the phase space was perturbed in such a way that every phase-space coordinate is changed, but the total energy remains fixed. The system is evolved for a time $\Delta t^* = 0.25$ ($\approx$0.5 ps) before the MLE is calculated using Eq. (2). The evolved perturbation is then projected along itself such that its magnitude equals that of the initial perturbation $|\delta\Gamma(0)|$ and the process is repeated up to 100 times. The MLE we calculated this way is insensitive to our choices of initial perturbation size $|\delta\Gamma(0)|$ and the evolution time Δt^* within reasonable ranges. The calculated values are then averaged to give the mean MLE *over a given trajectory*, $\overline{\Lambda}$. We calculate identical results for $\overline{\Lambda}$ (up to statistical fluctuations) under different initial conditions. This fact, combined with states neighboring in total energy having neighboring values of $\overline{\Lambda}$ means that the time averaged MLE, $\overline{\Lambda}$, and the phase average MLE, $\langle\Lambda\rangle$, are the same quantity. From here onward we shall not distinguish these two quantities and use the term MLE and symbol Λ to refer to them.

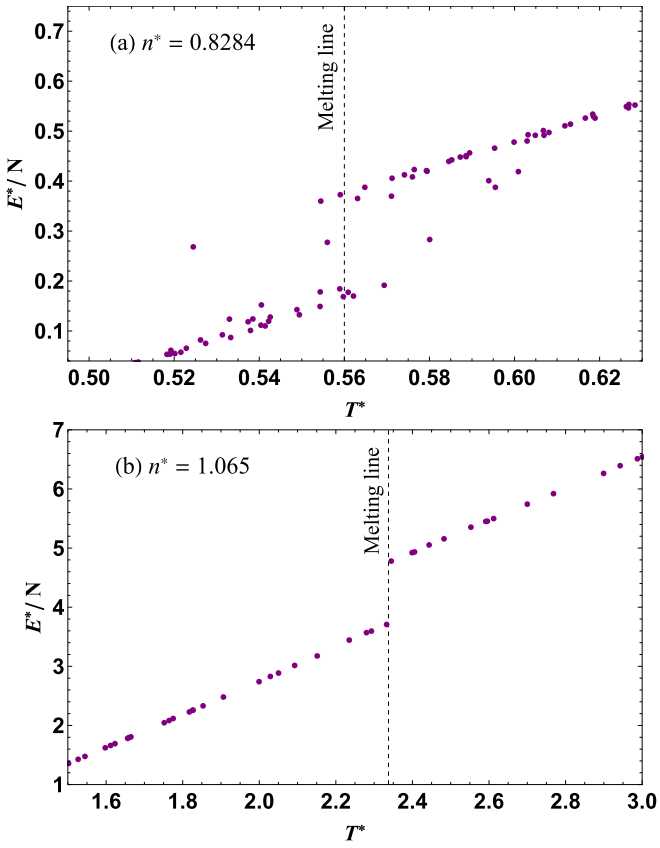

FIG. 3. Reduced energy per particle E^*/N across the melting line at reduced concentrations of (a) 0.8284 and (b) 1.065.

III. RESULTS AND DISCUSSION

We first discuss the transition at the melting line. Reduced energies as a function of reduced temperature are plotted in Fig. 3. The well-known discontinuity of energy across the melting line allows us to discern its location when we plot the MLE versus reduced energy in Fig. 4. We see the previously documented [28–31,34] discontinuity in the MLE in the transition from the solid to liquid phase. Dynamically speaking, the distinction between these phases is that liquids combine oscillation with diffusive jumps (in this sense the liquid is called a "dynamically mixed state" [13]). This was used by Nayak *et al.* to describe the discontinuity of the MLE in terms of the sudden expansion in the available phase space. This is a point we shall return to when we discuss the FL.

We plot VAFs in Fig. 5, indicating the FL determined by the disappearance of the minima. At lower densities, the disappearance of the minima happens fairly steadily. However, at the highest density, a very slightly minimum remains for a temperature range that spans almost 1000 K. The "zoomed-in" inset of Fig. 5 shows the gradual disappearance

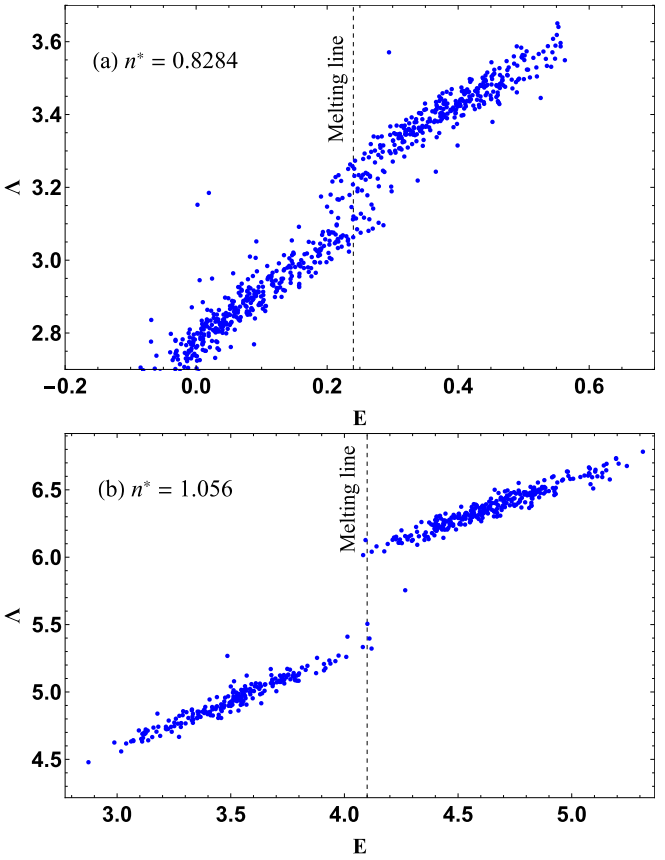

FIG. 4. Maximal Lyapunov exponent Λ across the melting line at reduced concentrations of (a) 0.8284 and (b) 1.065.

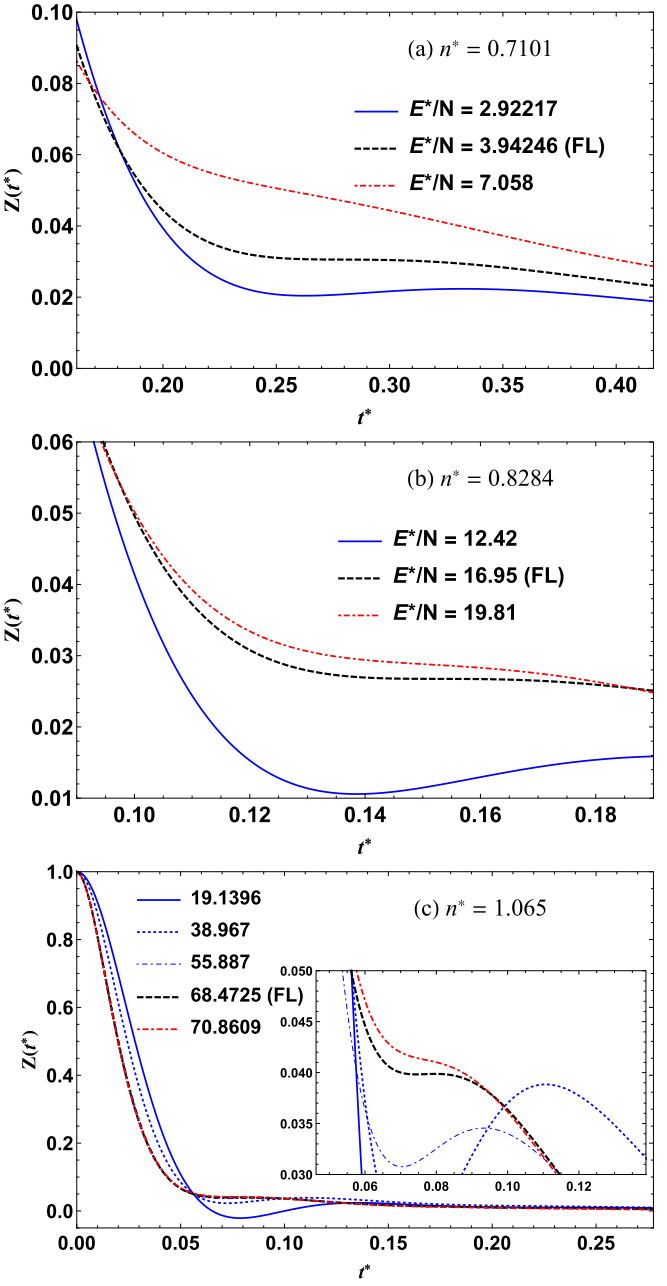

FIG. 5. Velocity autocorrelation functions as a function of reduced energy per atom and reduced time $Z(t^*)$ at the four different concentrations.

of this minimum—these VAFs are mostly indistinguishable at a lower resolution despite being at very different energies. This means that after most atomic oscillation is dispersed, a very slight component disappears far more gradually, which happens because the system density is fixed at a high value. In this sense, the system is almost completely diffusive and "gaslike" far before the disappearance of the minimum, and the last leg of the transformation takes place much more slowly. Energies and temperatures at the FL are listed in Table II.

Figure 6 plots the MLE as a function of reduced energy, up to and beyond the FL. We also include the thermodynamic definition of the FL, $c_V = 2$ [13], as an alternative marker of the dynamical crossover. The high-temperature functional dependence of the MLE is clearly visible with the logarithmic axes: $\Lambda = a(E^*)^b$. A power law with *temperature* for the MLE has been observed in a diverse range of condensed matter systems [41–43], though at far lower temperatures than those probed in this study. At lower densities, the crossover to this power-law relationship closely coincides with the both the dynamical crossover at the FL and the thermodynamic crossover at $c_V = 2$. At the highest density, the dynamical crossover occurs deep within this power-law regime. However, we note, as discussed above, a very small minimum in the VAFs disappears in the energy range of $E^*/N \approx 40$ to $E^*/N \approx 68$ (this is a larger range than that between the melting line and FL at the other densities), which corresponds to a very minor component of molecular oscillation disappearing in this range. For the most part, atomic oscillation gives way to diffusion at much lower energies than the disappearance of the minimum, represented in Fig. 6 by the gradual approach to the power-law relationship as oscillatory modes disappear.

The reason the crossover in the MLE at the FL is gradual rather than abrupt is because the crossover in dynamics is also gradual. Across the melting line, the particle dynamics abruptly gain an oscillatory character. A liquid just above the melting line has a finite relaxation time between diffusive "jumps," allowing it to support transverse collective modes below a certain wavelength [44–46]. As temperature is increased, the relaxation time becomes shorter, reducing

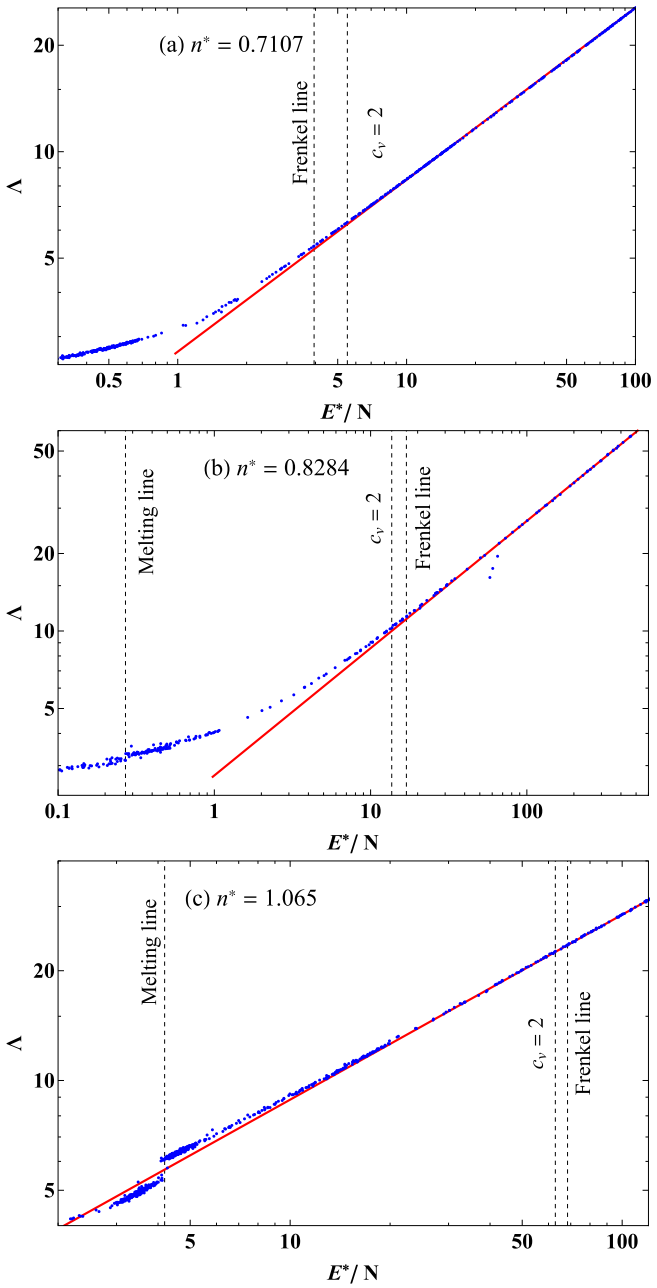

FIG. 6. Maximal Lyapunov exponent Λ in the fluid state at reduced concentrations of (a) 0.7107, (b) 0.8284, and (c) 1.056. The red lines are fitted power-law relationships $\Lambda = a(E^*)^b$, meant as visual guides.

the maximum wavelength of transverse modes and thereby decreasing the heat capacity due to a reduction of the degrees of freedom in the system [47]. As the relaxation time drops below the oscillation period (at the FL), all oscillatory motion is lost, the system becomes fully diffusive, and the transverse spectrum becomes empty. This is accompanied by a thermodynamic crossover. Below the FL, the decrease in heat capacity is caused by the loss of long wavelength transverse modes due to the increasing relaxation time, above the FL, the decrease in heat capacity is caused by the loss of short wavelength longitudinal modes as the mean free path increases [13]. In harmonic systems, this crossover takes place at a heat capacity of $c_V = 2$ (with units where $k_B = 1$). The thermodynamic and dynamic (VAF) criteria correspond closely here and in previous studies [12,48].

This interpretation allows us to make sense of our results here. Between the melting line and the FL, as the relaxation time decreases, the MLE increases with energy. The MLE increases because of the increased prevalence of diffusion events. Diffusion events involve an abrupt change in phase-space coordinates as an atom escapes from its local "cage" into another (see Fig. 1). These events are typically instigated by an atom's neighbors opening a low-energy pathway to form a neighboring cage with their thermal motion (the energy barrier of escape is lowered rather than the particle gaining the necessary energy to overcome the high barrier). We propose that these diffusion events are the liquid equivalent to "collisions" from kinetic theory because they involve a near-instantaneous decorrelation in particle coordinates and velocities and are sensitive to initial conditions (in the sense that an atom undergoes such an event because of transitory circumstances in its neighbors). The discontinuity of the MLE at the melting line is due to the sudden introduction of these events. This regime terminates smoothly as the relaxation time becomes comparable to the liquid oscillation period and a local rigid structure can no longer be defined. In other words the state becomes dynamically pure as atoms are continuously diffusing rather than doing so in opportunistic jumps (again see Fig. 1). The events of dynamic sensitivity are now the collisions of kinetic theory. Scattering is what makes the Lorentz gas a chaotic dynamical system [26]. These collisions now determine the evolution of the MLE without contribution from diffusion events, which is why it follows a single functional form. The collisions become more frequent with temperature at a fixed density. For a hard-sphere gas, the mean collision rate is [49]

$$w_{\text{coll}} = n\pi d^2 \sqrt{\frac{6k_B T}{m}}. \tag{5}$$

This is a concave function of temperature (and thus energy), which is a property exhibited by the MLE at all densities (the gradient in the log-log plots in Fig. 6 is less than unity). At the lower densities, this power-law regime spans more than an order of magnitude of energy above the FL. The fluid at the highest density, even well below the FL, is mostly dominated by diffusion and collisions, but there is a transitory period of oscillation for some molecules. We can interpret that collisions are responsible for the bulk of dynamical instability in these states, but a small fraction of atoms at any given time undergoing oscillation do not contribute to dynamical instability in this way. This crossover period of small deviation from the power law is much smaller at lower densities.

IV. CONCLUSIONS

We have presented a novel study of Lyapunov exponents which focuses on the supercritical fluid state. We find that the MLE in the "gaslike" deeply supercritical LJ system evolves with energy according to a single analytic function, which we explain in terms the fluid's dynamical evolution. Recent advances in the field of theoretical liquid physics

[13] have explained many liquid properties by describing the state in terms of two dynamical modes: molecular oscillation around quasiequilibrium positions and abrupt diffusion events between quasiequilibrium positions. Molecular oscillation terminates at the FL, and the dynamical evolution switches from a loss of oscillation to a decline of collisions. This dynamical crossover causes a crossover in both thermodynamics and structure in many different fluid systems [14–20]. On the basis of our MD simulations, this same dynamical crossover causes a crossover in the MLE. This crossover is seen power-law dependence of the MLE on energy above the FL and the deviation from this law below the FL. We explain this crossover in terms of diffusion events and collision events, prevalent below and above the FL respectively, which we propose are the major contributors to dynamical instability in these fluid states (as summarised in Fig. 1). The Lyapunov spectrum is linked to dynamics much more intimately than thermodynamics and structure and has been used in the past to indicate changes of phase [28–32,34,35]. Our results therefore do not only help understand microscopic chaos in the fluid state, but also show that the depiction of liquids as dynamically mixed states and the idea of the FL which separates regions in the supercritical part of the phase diagram are supported directly by properties of the classical phase space itself.

ACKNOWLEDGMENTS

I thank O. Dicks and K. Trachenko for insightful discussions, advice, and critical reading of the manuscript. This research utilized Queen Mary's Apocrita HPC facility, supported by QMUL Research-IT [50].

[1] R. Zwanzig, *Nonequilibrium Statistical Mechanics* (Oxford University Press, Oxford, 2001).

[2] J. R. Dorfman, *An Introduction to Chaos in Nonequilibrium Statistical Mechanics* (Cambridge University Press, Cambridge, UK, 1999).

[3] N. S. Krylov, *Works on the Foundations of Statistical Physics* (Princeton University Press, Princeton, NJ, 1980).

[4] P. Gaspard, *Chaos, Scattering and Statistical Mechanics* (Cambridge University Press, Cambridge, UK, 1998).

[5] H. A. Posch and W. G. Hoover, Lyapunov instability of dense Lennard-Jones fluids, Phys. Rev. A **38**, 473 (1988).

[6] J. R. Dorfman and P. Gaspard, Chaotic scattering theory of transport and reaction-rate coefficients, Phys. Rev. E **51**, 28 (1995).

[7] P. Gaspard and G. Nicolis, Transport Properties, Lyapunov Exponents, and Entropy Per Unit Time, Phys. Rev. Lett. **65**, 1693 (1990).

[8] D. J. Evans, E. G. D. Cohen, and G. P. Morriss, Viscosity of a simple fluid from its maximal Lyapunov exponents, Phys. Rev. A **42**, 5990 (1990).

[9] B. M. Boghosian, P. V. Coveney, and H. Wang, A new pathology in the simulation of chaotic dynamical systems on digital computers, Adv. Theory Simul. **2**, 1900125 (2019).

[10] G. E. Norman and V. V. Stegailov, Stochastic theory of the classical molecular dynamics method, Math. Models Comput. Simul. **5**, 305 (2013).

[11] V. V. Brazhkin, Yu. D. Fomin, A. G. Lyapin, V. N. Ryzhov, and K. Trachenko, Two liquid states of matter: A dynamic line on a phase diagram, Phys. Rev. E **85**, 031203 (2012).

[12] V. V. Brazhkin, Yu. D. Fomin, A. G. Lyapin, V. N. Ryzhov, E. N. Tsiok, and K. Trachenko, Liquid-Gas Transition in the Supercritical Region: Fundamental Changes in the Particle Dynamics, Phys. Rev. Lett. **111**, 145901 (2013).

[13] K. Trachenko and V. V. Brazhkin, Collective modes and thermodynamics of the liquid state, Rep. Prog. Phys. **79**, 016502 (2016).

[14] L. Wang, C. Yang, M. T. Dove, Yu. D. Fomin, V. V. Brazhkin, and K. Trachenko, Direct links between dynamical, thermodynamic, and structural properties of liquids: Modeling results, Phys. Rev. E **95**, 032116 (2017).

[15] L. Wang, C. Yang, M. T. Dove, V. V. Brazhkin, and K. Trachenko, Thermodynamic heterogeneity and crossover in the supercritical state of matter, J. Phys.: Condens. Matter **31**, 225401 (2019).

[16] C. Prescher, Yu. D. Fomin, V. B. Prakapenka, J. Stefanski, K. Trachenko, and V. V. Brazhkin, Experimental evidence of the Frenkel line in supercritical neon, Phys. Rev. B **95**, 134114 (2017).

[17] D. Smith, M. A. Hakeem, P. Parisiades, H. E. Maynard-Casely, D. Foster, D. Eden, D. J. Bull, A. R. L. Marshall, A. M. Adawi, R. Howie, A. Sapelkin, V. V. Brazhkin, and J. E. Proctor, Crossover between liquidlike and gaslike behavior in CH_4 at 400 K, Phys. Rev. E **96**, 052113 (2017).

[18] J. E. Proctor, C. G. Pruteanu, I. Morrison, I. F. Crowe, and J. S. Loveday, Transition from gas-like to liquid-like behavior in supercritical N_2, J. Phys. Chem. Lett. **10**, 6584 (2019).

[19] C. Cockrell, O. A. Dicks, V. V. Brazhkin, and K. Trachenko, Pronounced structural crossover in water at supercritical pressures, J. Phys.: Condens. Matter **32**, 385102 (2020).

[20] C. J. Cockrell, O. Dicks, L. Wang, K. Trachenko, A. K. Soper, V. V. Brazhkin, and S. Marinakis, Experimental and modeling evidence for structural crossover in supercritical CO_2, Phys. Rev. E **101**, 052109 (2020).

[21] T. Iwashita, D. M. Nicholson, and T. Egami, Elementary Excitations and Crossover Phenomenon in Liquids, Phys. Rev. Lett. **110**, 205504 (2013).

[22] G. G. Simeoni, T. Bryk, F. A. Gorelli, M. Krisch, G. Ruocco, M. Santoro, and T. Scopigno, The Widom line as the crossover between liquid-like and gas-like behavior in supercritical fluids, Nat. Phys. **6**, 503 (2010).

[23] N. P. Kryuchkov, L. A. Mistryukova, A. V. Sapelkin, V. V. Brazhkin, and S. O. Yurchenko, Universal Effect of Excitation Dispersion on the Heat Capacity and Gapped States in Fluids, Phys. Rev. Lett. **125**, 125501 (2020).

[24] T. J. Yoon, M. Y. Ha, E. A. Lazar, W. B. Lee, and Y. W. Lee, Topological characterization of rigid-nonrigid transition across the Frenkel line, J. Phys. Chem. Lett. **9**, 6524 (2018).

[25] L. Xu, P. Kumar, S. V. Buldyrev, S.-H. Chen, P. H. Poole, F. Sciortino, and H. E. Stanley, Relation between the Widom line and the dynamic crossover in systems with a liquid-liquid phase transition, Proc. Nat. Acad. Sci. USA **102**, 16558 (2005).

[26] L. A. Bunimovich and Ya G. Sinai, Markov partitions for dispersed billiards, Commun. Math. Phys. **78**, 247 (1980).

[27] H. A. Posch and W. G. Hoover, Equilibrium and nonequilibrium Lyapunov spectra for dense fluids and solids, Phys. Rev. A **39**, 2175 (1989).

[28] S. K. Nayak, R. Ramaswamy, and C. Chakravarty, Maximal Lyapunov exponent in small atomic clusters, Phys. Rev. E **51**, 3376 (1995).

[29] V. Mehra and R. Ramaswamy, Curvature fluctuations and the Lyapunov exponent at melting, Phys. Rev. E **56**, 2508 (1997).

[30] Ch. Dellago and H. A. Posch, Kolmogorov-Sinai entropy and Lyapunov spectra of a hard-sphere gas, Physica A **240**, 268 (1997).

[31] K. H. Kwon and B. Y. Park, Lyapunov exponent and the solid-fluid phase transition, J. Chem. Phys. **107**, 5171 (1997).

[32] P. Butera and G. Caravati, Phase transitions and Lyapunov characteristic exponents, Phys. Rev. A **36**, 962 (1987).

[33] G. M. Tanner, A. Bhattacharya, S. K. Nayak, and S. D. Mahanti, Dynamics of melting argon clusters, Phys. Rev. E **55**, 322 (1997).

[34] S. K. Nayak, P. Jena, K. D. Ball, and R. S. Berry, Dynamics and instabilities near the glass transition: From clusters to crystals, J. Chem. Phys. **108**, 234 (1998).

[35] J. Barré and T. Dauxois, Lyapunov exponents as a dynamical indicator of a phase transition, Europhys. Lett. **55**, 164 (2001).

[36] C. Yang, M. T. Dove, V. V. Brazhkin, and K. Trachenko, Emergence and Evolution of the K Gap in Spectra of Liquid and Supercritical States, Phys. Rev. Lett. **118**, 215502 (2017).

[37] I. T. Todorov, W. Smith, K. Trachenko, and M. T. Dove, DL_POLY_3: New dimensions in molecular dynamics simulations via massive parallelism, J. Mater. Chem. **16**, 1911 (2006).

[38] M. P. Allen and D. J. Tildesley, *Computer Simulation of Liquids*, Vol. 57 (Clarendon Press, London, 1991).

[39] C. S. Barrett and L. Meyer, X-ray diffraction study of solid argon, J. Chem. Phys. **41**, 1078 (1964).

[40] G. Benettin, L. Galgani, and J. M. Strelcyn, Kolmogorov entropy and numerical experiments, Phys. Rev. A **14**, 2338 (1976).

[41] M. Colonna and A. Bonasera, Lyapunov exponents in unstable systems, Phys. Rev. E **60**, 444 (1999).

[42] W. Nan, W. Xi-Zhen, L. Zhu-Xia, W. Ning, Z. Yi-Zhong, and S. Xiu-Quan, Behavior of the Lyapunov exponent and phase transition in nuclei, Chin. Phys. Lett. **17**, 711 (2000).

[43] M. Foroutan, A. H. Jalili, and Z. Nikouei, Determination of the maximal Lyapunov exponent through the effective potential energy: Exact phase transition temperature of few particle system CF_4, J. Phys. Soc. Jpn. **78**, 124003 (2009).

[44] J.-P. Boon and S. Yip, *Molecular Hydrodynamics* (Dover, London, 1991).

[45] U. (Umberto) Balucani and M. Zoppi, *Dynamics of the Liquid State* (Clarendon Press, London, 1994).

[46] J.-P. Hansen and I. R. McDonald, *Theory of Simple Liquids* (Elsevier Academic Press, Amsterdam, 2006).

[47] D. Bolmatov, V. V. Brazhkin, and K. Trachenko, The phonon theory of liquid thermodynamics, Sci. Rep. **2**, 421 (2012).

[48] N. P. Kryuchkov, L. A. Mistryukova, V. V. Brazhkin, and S. O. Yurchenko, Excitation spectra in fluids: How to analyze them properly, Sci. Rep. **9**, 10483 (2019).

[49] S. Blundell and K. M. Blundell, *Concepts in Thermal Physics* (Oxford University Press, Oxford, 2010).

[50] T. King, S. Butcher, and L. Zalewski, Apocrita - High Performance Computing Cluster for Queen Mary University of London Zenodo, doi: 10.5281/zenodo.438045 (2017).